IEEE Access
Multidisciplinary | Rapid Review | Open Access Journal

Received November 17, 2019, accepted December 3, 2019, date of publication December 12, 2019,
date of current version December 23, 2019.

Digital Object Identifier 10.1109/ACCESS.2019.2959004

Blur Feature Extraction Plus Automatic KNN Matting: A Novel Two Stage Blur Region Detection Method for Local Motion Blurred Images

MINGHUA ZHAO[1,2], DAN LI[1], ZHENGHAO SHI[1], SHUANGLI DU[1], PENG LI[1], AND JING HU[1]

[1]School of Computer Science and Engineering, Xi'an University of Technology, Xi' an 710048, China
[2]Shaanxi Key Laboratory of Network Computing and Security Technology, Xi' an 710048, China

Corresponding author: Minghua Zhao (mh_zhao@126.com)

This work was supported in part by the National Key Technology Research and Development Program of China under Grant 2017YFB1402103-3, in part by the National Natural Science Foundation of China under Grant 61401355 and Grant 61602373, in part by the Key Laboratory Foundation of Shaanxi Education Department, China, under Grant 14JS072, in part by the Natural Science Foundation of Shaanxi province, China under Grant 2019JM-381, and in part by the Science and Technology Project of Xi'an City under Grant 2017080CG/RC043(XALG011), Grant 2017080CG/RC043 (XALG027), and Grant 2017080CG/RC043(XALG021).

ABSTRACT To deal with the serious visual artifacts caused by the consistent restoration algorithm on local motion blurred images, a novel two stage blur region detection method including coarse location and region refinement for local blurred images is proposed in this paper. First, blur feature discriminant criteria in frequency domain and spatial domain is defined to generate blur feature image; then, binarization is used on the blur feature image to obtain the coarse blur region detection map; subsequently, morphological methods are used to process the clear and blur areas and the trimap is obtained. Finally, the refinement detection of blur region is achieved by combination of the trimap and automatic KNN matting algorithm. Experimental results show that the proposed algorithm can detect the local blurred region quickly and effectively, and it has outperformed other traditional methods in the application of blur region detection and image restoration as well.

INDEX TERMS Image processing, image restoration, image quality, local blur feature, blur feature extraction, KNN matting.

I. INTRODUCTION

Local blur of images are common and can be caused by various reasons, such as dirty camera cover, incomplete level of camera sensor, inaccurate camera focus and moving objects et.al. Compared with other reasons, local blur caused by image motion is very common. In many scenarios such as detection and tracking of fast targets [1], velocity estimation [2], [3], scene classification [4], motion segmentation [5] and image segmentation [6] etc. Local motion blurred regions will cause very serious interference and are essential to be removed. Therefore, it is very important to detect local motion blurred regions automatically.

The associate editor coordinating the review of this manuscript and approving it for publication was Habib Ullah.

To achieve automatic detection of local motion blurred regions, the following two issues need to be deliberated. First, what kind of features can be used to describe motion; second, how to automatically achieve the accurate detection of motion blurred regions. For the first issue, it is very difficult to make accurate feature representation without knowing the motion state of a moving object. For the second issue, as an ill-posed sub-problem in image segmentation, the accuracy of automatic region detection results rely heavily on the accurate representation of features in the first issue.

There are many developments about the research of local motion blurred region detection [7]–[9] in recent years. The existing traditional blur region detection methods can be divided into four categories. The first category is local motion blurred region detection algorithm based on singular value

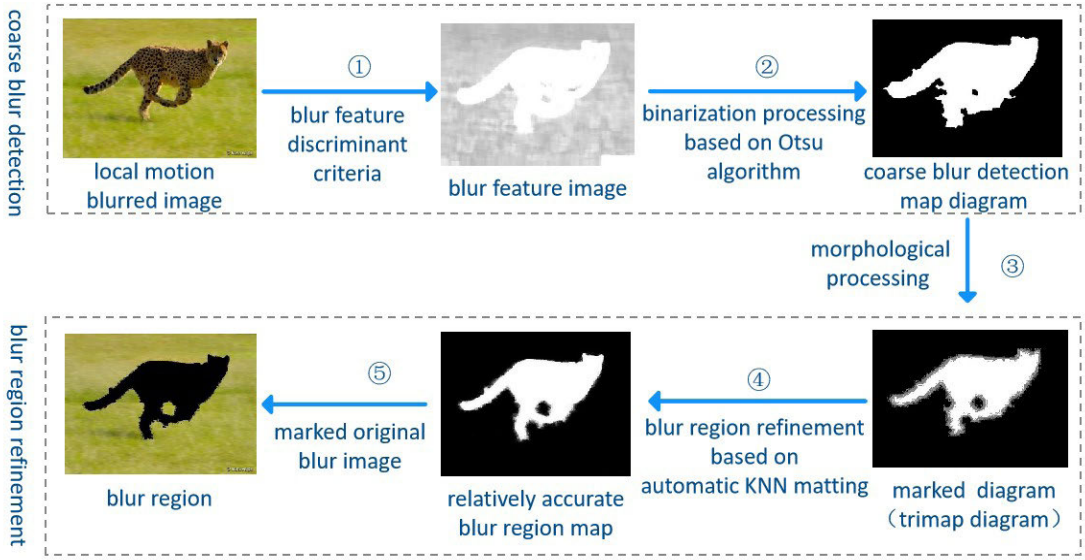

FIGURE 1. Framework of the proposed algorithm.

feature. Su *et al.* [10] found that larger singular values in the image singular value vector are mainly used to represent image structure, shape and other general information, while the smaller singular values are mainly used to represent image texture and other image details. Therefore, the blur region detection was carried out according to the proportion of the larger singular values to all the singular values. However, because some flat clear areas may contain less image details and may have singular value features similar to motion blurred areas, some detection results may inevitably be misjudged. The second category is local motion blurred region detection algorithm based on Bayesian classifier. This kind of methods extract motion blur features and then construct a Bayesian classifier for detection. Liu *et al.* [11] extracted features by combining information of power spectrum, saturation, gradient and color of the image, and then used the extracted features to construct a Bayesian classifier for region detection. Shi *et al.* [12] extracted blur features such as heavy-tailed distribution, kurtosis, power spectrum and linear filtering by combining gradient distribution, power spectrum and local filter of the image, and constructed a blur confidence mapping in multi-scale space based on all these blur features. Then, naive Bayes classifier was used for blur region detection. This method [12] may achieve a good blur region detection effect, but the proposed blur features were relatively complex and the extraction of the blur features was time consuming. The third category is motion blurred region detection algorithm based on blur kernel estimation. This algorithm first estimates the blur kernel and then performs blur detection according to the characteristics of the blur kernel. Bahrami *et al.* [13] estimated the local blur kernel according to image patches and then measured the relative blur degree of local blur kernel with reblurring technology, according to which, blur image patches and sharp image patches were classified. Wang *et al.* [14] conducted blur kernel estimation and image segmentation by alternating iteration. The fourth category method is motion blurred region detection algorithm based on image matting technology. This kind of algorithm carries on the coarse blur region detection according after blur feature extraction and then detects blur region using the matting algorithm finely. Dai and Wu [15] regarded local blur images as two layers of foreground and background according to clear and blur areas and achieved the detection of blur areas by combining image matting technology, user mark and appropriate image prior model. Kohler *et al.* [16] used the existing blind deconvolution method to estimate blur kernel for the coarse blur region manually calibrated by the users, and then guided the refinement of the blur region by combining the estimated blur kernel information with the lazy matting algorithm. However, most existing methods often require additional information such as user interaction or prior knowledge to achieve satisfactory detection performance. Zhao *et al.* [17] conducted blur region detection by combining Gaussian mixture model (GMM), local standard deviation and maximum color saturation and then used lazy matting method to extract blur areas. This method could achieve better blur area detection effect. However, the blur region detection model was complex and the edge of blur area detected based on the improved lazy matting algorithm was not very accurate.

Compared with the first three categories of blur region detection methods, the fourth category is more accurate and the edge detection effect of blur region is better. Therefore, the fourth category is adopted and a local motion blurred region detection algorithm based on blur feature extraction and automatic k-nearest neighbor (KNN) matting is proposed in this paper, as shown in figure 1. First, a novel blur feature discriminant criteria in both frequency domain and spatial

domain is defined to generate blur feature image; second, Otsu algorithm is used to the binarization processing for the blur feature image to generate coarse blur detection image; third, morphological processing is used to deal with the clear and blur areas in the coarse blur detection image, based on which, the original blur image is marked to get the corresponding three sub-map(trimap). Finally, the refinement detection of blur region is achieved by combination of the trimap and improved KNN matting algorithm [18].

The structure and organization of the paper is as follows: **In Section 1**, the general framework of the algorithm is presented based on the summary of existing blur region detection algorithms. **In Section 2**, the blur features including spatial domain and frequency domain are discussed and extracted. **In Section 3**, the blur region detection algorithm composed of coarse blur region detection and fine blur region detection is proposed. **In Section 4**, experiments are carried out and the proposed method is evaluated. **In Section 5**, conclusions and discussions are provided.

II. BLUR FEATURE DISCRIMINANT CRITERIA IN FREQUENCY DOMAIN AND SPATIAL DOMAIN

Blurring is an overall visual effect of local areas and so an image is divided into patches by sliding window, based on which, the blur feature of each image patch is used to represent the blur characteristics of the central pixel position of the image patch. Blur feature discriminant criteria in frequency domain and spatial domain is defined and used to extract blur features for local motion blurred image region detection.

A. BLUR FEATURE EXTRACTION IN FREQUENCY DOMAIN FEATURE

Compared with clear image, blur image ignores most of the image details and only contains the overview image information. From the perspective of frequency domain, an image may lose most high-frequency information by convolution operation which can make a clear image to a blurred one. Therefore, the sum and mean of the fast Fourier spectrum of a blurred image are lower than that of a clear image. Blur feature named average energy value is used to represent the blur characteristics in frequency domain, which is defined as equation (1).

$$q_1 = \frac{\sum_{i=0}^{k}\sum_{j=0}^{k}\log(abs(Fc(i,j)))}{k \times k} \tag{1}$$

where F_c denotes the spectrograph obtained by fast central Fourier transform of image I, abs(x) denotes modulus of complex number x, log(x) denotes the logarithm of x, and k × k denotes the size of the image patch.

The main steps of blur feature extraction in frequency domain can be summarized as follows:

Firstly, a blurred image patch p(x, y) is input;

Secondly, the fast Fourier transform of the blur image patch p(x, y) is taken to get the spectrograph F;

Thirdly, the origin of spectrograph F is moved to the center of the image to get image F_c;

Fourthly, modular operation and logarithm operation are taken on image F_c to get lgF.

Finally, the pixel values of lgF are averaged to obtain the blur feature value of the central pixel of image patch p(x, y) in frequency domain.

B. CONTRAST-COLOR SATURATION FEATURE EXTRATION IN SPATIAL DOMAIN

For comprehensive and accurate measure of the blur degree of an image, a spatial domain feature named contrast-color saturation is defined as equation (2) and used for blur detection.

$$q_2 = \frac{C_p}{SS} \tag{2}$$

In equation (2), C_p denotes image contrast and SS denotes image color saturation slope.

1) IMAGE CONTRAST

Local motion blur is a state in which the local details of an image are not clear due to the weighted stacking of pixels in the local area caused by the movement. The most direct influence of this process is the maximum and minimum of pixel intensity for an image patch. Image contrast is defined as equation (3).

$$C_p = \frac{P_{max} - P_{min}}{P_{max} + P_{min}} \tag{3}$$

In equation (3), P_{max} and P_{min} denotes the maximum and minimum value of pixel intensity for a blurred patch respectively. From the definition of image contrast, it can be concluded that the more blurred the image is, the lower the contrast value is. The main reason is that blurred image patch will cause smaller difference between pixel intensities.

2) COLOR SATURATION SLOPE

The blurring process will reduce the color saturation of the image. The divergence degree between the maximum saturation of the local image patch and the maximum saturation of the whole image is used to measure the blur degree of the local blurred image and is named as the color saturation slope, which is defined as equation (4).

$$\mathrm{SS} = \frac{\max\limits_{x\in I} S(I)(x) - \max\limits_{y\in p} S(p)(y)}{\max\limits_{x\in I} S(I)(x)} \tag{4}$$

In equation(4), p denotes the blur image patch, I denotes the whole blur image, S(I)(x) denotes the color saturation value of pixel x in image I, and maxS(I)(x) denotes the maximum color saturation value of image I, which is defined as equation(5) [19].

$$\mathrm{S}(I)(x) = 1 - \frac{3}{\operatorname{sum}\limits_{c\in\{r,g,b\}} I^c(x)} minI^c(x) \tag{5}$$

In equation (5), x denotes the pixel point position of image I, and I_c denotes the c-th color channel of image I.

From the definition of saturation slope, it can be concluded that the more blurred the image is, the greater difference of color saturation between the image patch and the whole image is, which will cause higher color saturation slope.

The main steps of blur feature extraction in spatial domain can be summarized as follows:

Firstly, a blurred image patch p(x, y) and an original blurred image I(x, y) are input.

Secondly, equation (4) is used to calculate the color saturation slope value SS of image patch p(x, y).

Thirdly, the image patch p(x, y) is converted into grayscale image, and the contrast value C_p of the image patch is calculated using equation (3).

Fourthly, the blur feature q_2 of image patch p(x, y) is calculated using equation (2).

Finally, q_2 is set as the blur feature value of the central pixel of image patch p(x, y) in spatial domain.

In order to comprehensively denote the blur characteristics, blur feature is defined as equation (6) for local blurred region extraction by combining the features in frequency domain and spatial domain.

$$q = \alpha q_1 + \beta q_2 \tag{6}$$

In equation (6), α and β are the weight of blur feature q_1 and q_2, respectively. If we treat the blur feature q as unit 1, then the weight parameter of α and β have the following relationship:

$$\alpha + \beta = 1 \tag{7}$$

III. BLUR REGION DETECTION

Blur region detection can be divided into coarse blur region detection and fine blur region detection.

A. COARSE BLUR REGION DETECTION BASED ON BLUR FEATURES

Coarse blur region detection has 4 steps:

Step 1: The blurred image shown in figure 2(a) is divided into patches according to the sliding window with size of k*k and step size of 1, as shown in figure 3. In figure 3, the arrows and the numbers indicate the direction of the window sliding and the three adjacent colored dashed blocks represent the obtained image patches by sliding the window.

Step 2: For each image patch, blur feature is obtained using equation (6) and used for denoting blur characteristics of the central pixel, based on which, the blur feature image is obtained, whose position in the original image is shown as S in figure 3.

Step 3: The blur feature image is extended to the same size as the original image by copying the pixel value of the outer edge, which is shown in figure 2(b).

Step 4: Otsu algorithm is used to calculate the binary threshold of blur feature image and the blur feature image is binarized to obtain the coarse blur region detection result, as shown in figure 2(c).

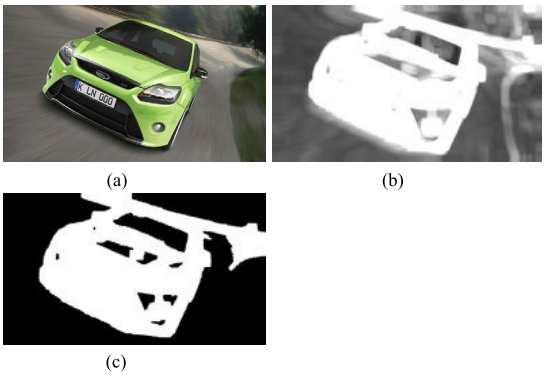

FIGURE 2. Coarse blur region detection process. (a) Local motion blur image; (b) Blur feature image; (c) Coarse blur detection result.

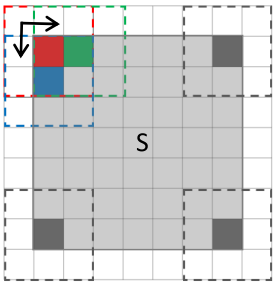

FIGURE 3. The sliding window diagram.

B. FINE BLUR REGION DETECTION BASED ON AUTOMATIC KNN MATTING ALGORITHM

Most of the blur regions can be detected by coarse blur detection step, but there is a small part of blur region boundary that cannot be detected successfully and the edge detection of the blur region is not accurate. Therefore, it is necessary to achieve accurate detection of blur region.

Regarding the local motion blur image as two layers of foreground and background, the idea of image matting [9], [13] can be used to achieve fine blur region detection.

Image matting refers to the problem of decomposing an image into two layers of foreground and background, which can be abstracted into the following equation:

$$I = \tau F + (1 - \tau) B \tag{8}$$

where I is the given image, F, B denotes the unknown foreground and background layer respectively, and the $\boldsymbol{\tau}$ is the unknown matte.

In the implementation of image matting problem, the original image is generally divided into three parts: determining foreground region, determining region and unknown region (named as trimap). The image matting method assumes that the value of $\boldsymbol{\tau}$ for each unknown pixel is a linear combination of its ''peripheral pixels'' and it can be obtained using the values of the determining regions iteratively. This problem is a serious ill-conditioned problem, some additional constraints need to be added to get a solution.

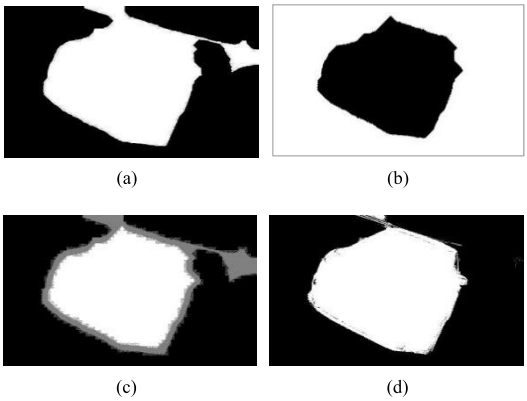

FIGURE 4. Fine blur region detection process. (a) Foreground region map; (b) Background region map; (c) Trimap diagram; (d) Relatively accurate blur region map.

KNN matting is an image matting algorithm with good visual performance and best MSE (Mean Square Error) [10]. In KNN matting, some user markups are used as trimap to solve the ill-conditioned problem.

In our method, we regard the clear area as the foreground and the blur area as the background respectively. Taking the coarse blur detection results as the trimap, KNN-matting is used to achieve the fine blur area detection quickly and effectively.

Fine blur region detection based on KNN matting has the following 4 steps.

Step 1: Morphological process including dilation and erosion are used on the coarse blur region detection result to obtain the background region map and the foreground region map, as shown in figure 4(a) and figure 4(b).

Step 2: The original image is marked according to the foreground and background labeling map and the trimap composed of foreground, background and unknown area is obtained, as shown in figure 4(c). In the traditional image matting algorithms, the trimap diagram is acquired by interactive user manual calibration.

Step 3: Taking the trimap diagram as a prior knowledge, the KNN matting algorithm is used automatically to refine the coarse blur detection map to determine the foreground proportion value of gray undetermined area in figure 4(c), as a result of which, the relatively accurate blur region map is obtained, as shown in figure 4(d).

Step 4: The blur region map is used to mark the original blur image, and the final clear region and blur region are separated, as shown in figure 5(b) and figure 5(c).

IV. EXPERIMENTS AND ANALYSIS

Motion blur images in the data set of literature [12] are used in the experiment to evaluate the performance of the proposed algorithm. In the following experiments, the values of feature extraction parameters α and β are set as 0.5 and the size of feature extraction image patches is 21×21. The experiments were conducted in the system environment of Windows10 64bit, Intel(R) Core(TM) i5-6200u CPU, 8GB memory and MATLAB R2016b.

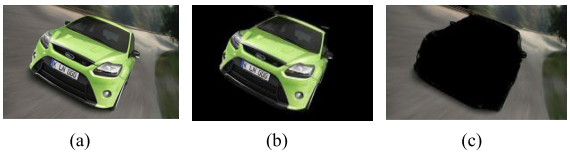

FIGURE 5. Blur region refinement effect schematic diagram. (a) Original blur image; (b) The separated clear region; (c) The separated blur region.

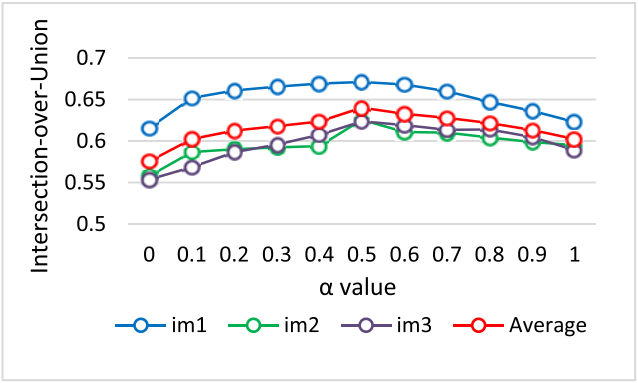

FIGURE 6. IoU values with different α.

A. DETERMINATION OF α AND β

Intersection-over-Union (IoU) is used to determine the values of α and β. IoU is a concept in target detection. It is the overlap rate of detected candidate regions and the ground truth, namely the ratio of their intersection to union. The larger the ratio value is, the higher the accuracy of the detection will be. Ideally, when the two are completely coincident, the ratio is 1. By calculating the IoU of the obtained coarse blur region detection result and the ground truth, the values α and β can be determined. The IoU results corresponding to different α values are shown as figure 6. In figure 6, im1, im2 and im3 corresponds to the three blurred images in figure 7 respectively, "Average" are the average value of im1, im2 and im3. From figure 6, we can see that when the value of α is less than 0.5, the accuracy rate of the coarse blur detection results is gradually improved with the increase of α. When α value is greater than 0.5, the accuracy rate of coarse blur detection results shows a gradual decline with the increase of α. When α is set as 0.5, the values of IoU are always the maximum, which shows the accuracy rate of coarse blur detection results. Because $\alpha+\beta=1$, the corresponding value of β also is 0.5. That is, we can conclude that when the two values are set as 0.5, we can get the best coarse blur detection result.

B. BLUR FEATURE EXTRATION PERFORMANCE IN FREQUENCY DOMAIN

Lena images with different degrees of blur shown as figure 8 are used to evaluate the effectiveness of the proposed blur feature extraction method in frequency domain. Figure 8 (a) is the original Lena image, figure 8 (b)$\sim$(f) are the blurred images obtained by moving the image with distance of 11 pixels, 15 pixels, 19 pixels, 21 pixels and 27 pixels

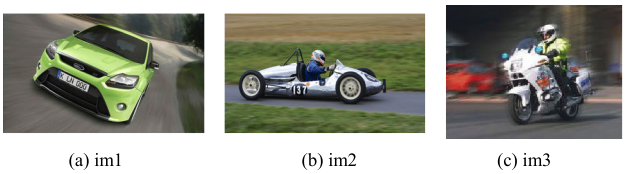

(a) im1 (b) im2 (c) im3

FIGURE 7. Motion Blurred images used in figure 6.

(a) (b) (c) (d) (e) (f)

FIGURE 8. Blurred images obtained by moving Lena with different distance. (a) Original image; (b) Len =11; (c) Len = 15; (d) Len = 19; (e) Len =21; (f) Len = 27.

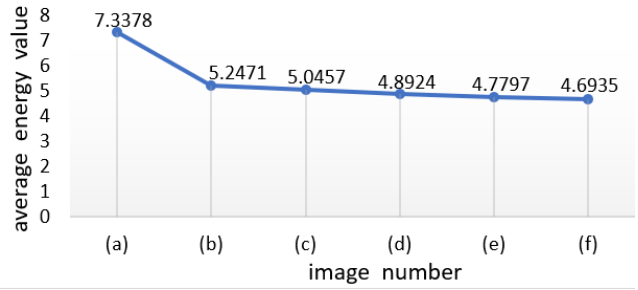

FIGURE 9. Average energy values of figure 8 (a) ∼ (f).

respectively. The corresponding average energy values of the center Fourier spectrum calculated by equation (1) are shown in figure 9. As can be seen from figure 9, compared with the clear image, the average energy value of the blur image is greatly reduced, meanwhile the difference between the average energy values of the blur images with different blur degree is small. That is, the proposed blur feature extraction method in frequency domain can effectively represent blur characteristics of an image.

C. BLUR FEATURE EXTEATION PERFORMANCE IN SPATIAL DOMAIN

1) BLUR FEATURE OF CONTRAST

Blurred images obtained by moving Lena with different distance are used to evaluate the effectiveness of the proposed contrast feature extraction method. The histograms corresponding to figure 8 (a) ∼ (f) are shown as figure 10, where the maximum and minimum values of pixel intensity for each image are marked with green dotted lines. As can be seen

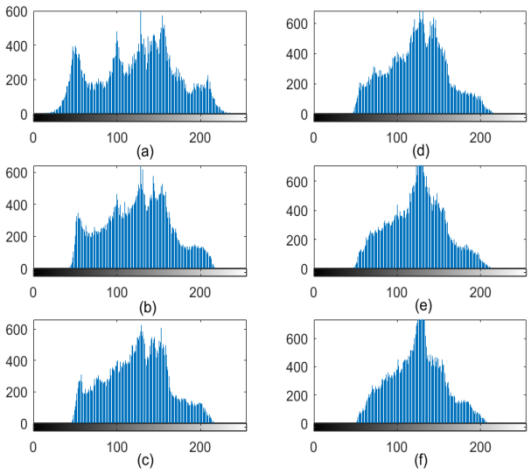

FIGURE 10. Histograms corresponding to figure 8(a) ∼ (f).

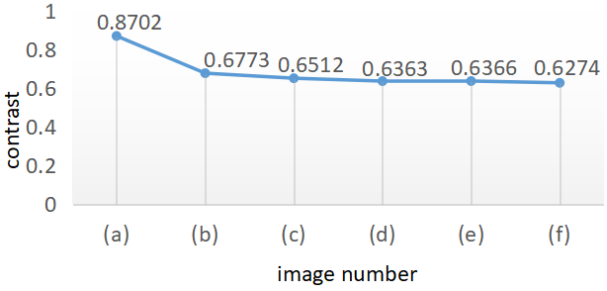

FIGURE 11. Contrast values corresponding to figure 8(a) ∼ (f).

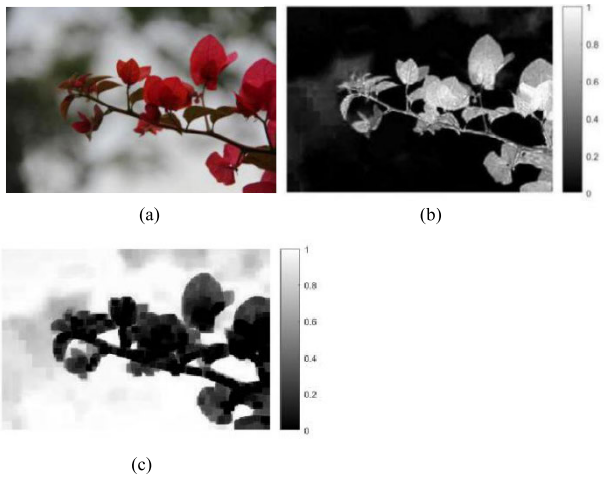

(a) (b) (c)

FIGURE 12. Blur feature of color saturation slope. (a) Local blur image; (b) The corresponding color saturation map of image (a); (c) Color saturation slope map corresponding to image (a).

from figure 10, the process of producing a blurred image by convolution operation on a clear image will lead to a decrease in the maximum and an increase in the minimum pixel intensity, and the difference between the maximum and minimum pixel intensity of different blur images is small. Figure 11 shows the contrast values corresponding to figure 8 (a) ∼ (f). As can be seen from figure 11, compared with clear image, blur images has smaller contrast values and

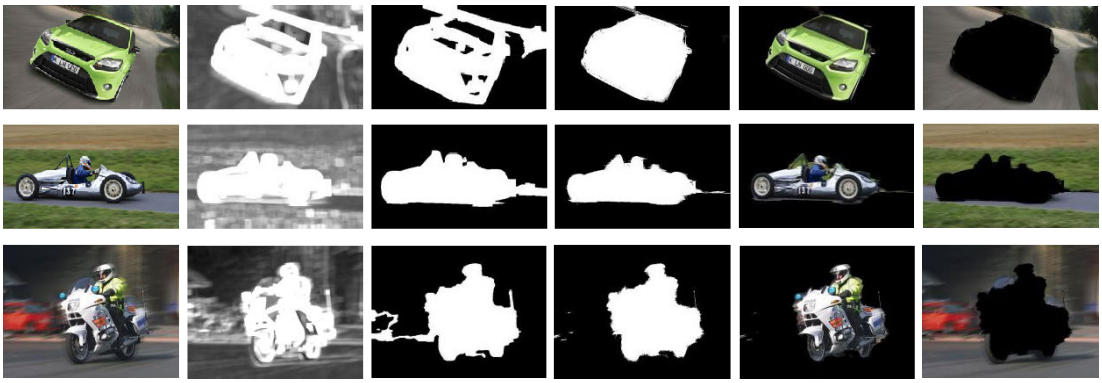

FIGURE 13. Blur region detection results. (a) Input blurred images; (b) Blur feature images; (c) Coarse blur region detection results; (d) Accurate blur region detection results; (e) The separated clear regions; (f) The separated blur regions.

the difference between contrast values of blur images with different blur degrees is small. Therefore, it is reasonable to use contrast as one of the criteria for blur detection of the image in the spatial domain, and it is also verified that contrast is inversely proportional to the blur degree of an image.

2) BLUR FEATURE OF COLOR SATURATION SLOPE

A local blurred image is used to evaluate the effectiveness of the proposed color saturation slope feature extraction method, as shown in figure 12. Figure 12(a) is a local blurred image, figure 12(b) is the corresponding color saturation map of figure 12(a), and figure 12(c) is the color saturation slope map corresponding to figure 12(a). As can be seen from figure 12(b), the higher saturation values are mainly distributed in the sharp and clear areas. As can be seen from figure 12(c), the higher color saturation slope values are mainly distributed in the flatter blur area, and the difference between color saturation slope values of the clear and blur area is obvious. Therefore, it is reasonable to use color saturation slope measure the blur characteristics in the spatial domain. It is also verified that the color saturation slope value is in direct proportion to the blur degree of the image. In conclusion, the proposed comprehensive spatial blur feature shown as equation (2) which is in direct proportional to contrast feature and inversely proportional to color saturation slope feature is significant for blur feature extraction.

D. BLUR REGION DETECTION EFFECT OF OUR PROPOSED METHOD

Three local motion blurred images are used to evaluate the effectiveness of the proposed blur region detection method. Figure 13(a) are three different local motion blurred images. Figure 13(b) are the blur feature images obtained by our proposed algorithm. It can be seen that the proposed blur features can well represent blur characteristics of images. Figure 13(c) are the coarse blur detection results obtained by using the proposed coarse blur detection method. It can be seen that the proposed coarse blur detection algorithm can detect most of the blur regions. Figure 13(d) are the accurate blur region detection results obtained by the proposed fine blur detection method. It can be seen that the blur region refinement method improves the results of coarse blur detection, eliminating most of the regional misclassification in coarse blur detection results and refining the edges of blur regions. Figure 13(e) and (f) are the separated clear areas and blur areas with our blur detection algorithm. As can be seen from the clear and blur areas, the detection effect of the proposed blur detection algorithm is relatively accurate.

E. BLUR REGION DETECTION RESULTS BY DIFFERENT METHODS

Three local blur images are used to evaluate the visual performance of our proposed method and other blur area detection methods [10]–[12], as shown in figure 15. Figure 14(a) are three different local motion blurred images. Figure 14(b) are the blur detection results by the method proposed by Su *et al.* [10]. Figure 14(c) are the blur detection results by the method proposed by Liu *et al.* [11]. Figure 14(d) are the blur detection results by the method proposed by Shi *et al.* [12]. Figure 14(e) are the blur detection results by our proposed method. Figure 14(f) are the ground truths. As can be seen from figure 14, the blur detection results obtained by the proposed algorithm are more outstanding than other methods in various complex situations. Meanwhile, the detection results obtained by our proposed algorithm are very close to the manual marked ground truth.

To quantitative analyze the effectiveness of the proposed method, 296 motion blurred images from the Blur Detection Dataset of Shi *et al.* [12] are used to obtain the precision-recall curves to compare our method and the other three methods [10]–[12], as shown in figure 15. We can see from figure 15 that our proposed method achieves the maximum precision within almost the whole recall range [0, 1]. This is mainly due to coarse blur region detection based on the combination of spatial domain with frequency domain, as well as the automatic fine blur region detection based on improved KNN matting.

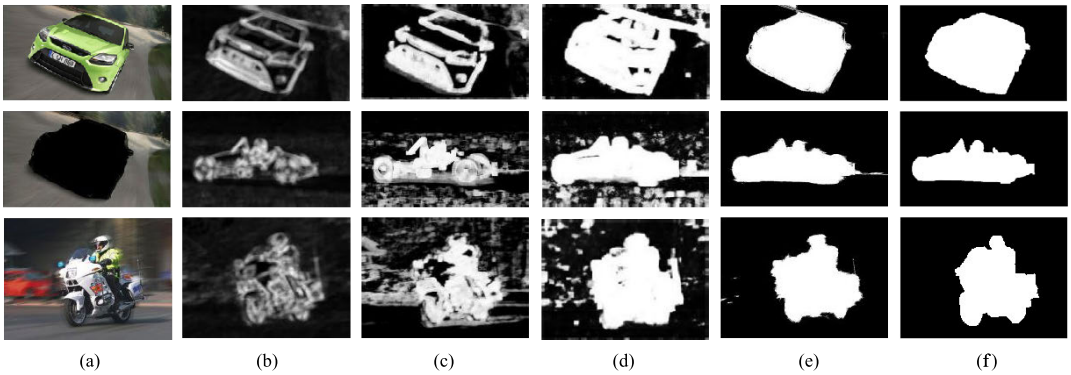

FIGURE 14. Blur region detection results by different methods. (a) Input local blurred images; (b) Blur detection results of Su's method [10]; (c) Blur detection results of Liu's method [11]; (d) Blur detection results of Shi's method [12]; (e) Blur detection results of our proposed method; (f) Ground truth.

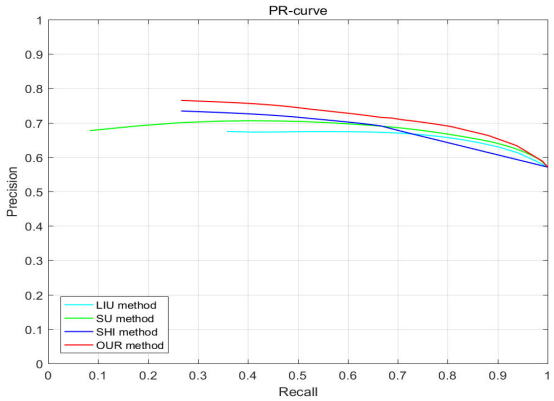

FIGURE 15. Precision-recall curves for different methods.

TABLE 1. Computational efficiency of different methods.

	Methods	Patch size	im1	im2	im3
Feature extraction time(s)	literature [12]	k=11	40	37	44
		k=15	63	58	73
		k=21	106	102	140
	Ours	k=21	30	28	34
Optimization time (s)	literature [12]		35	40	54
	Ours		6	5	7
Total time(s)	literature [12]		244	237	311
	Ours		36	33	41

F. COMPUTATIONAL EFFICIENCY OF DIFFERENT METHODS

The three motion blur images shown in Figure 14(a) are used to evaluate the effectiveness of the proposed blur region detection method in time efficiency and the three images are named as im1, im2 and im3. Table 1 shows the running time of the proposed method and the method in [12]. For the proposed method, optimization time refers to the time spent in the process of blur region refinement. As can be seen from table 1, the model in literature [12] extracted local blur features from three different scales. Given an input image, for each scale, they divided the image into patches and compute local blur feature corresponding to them. Meanwhile, the local blur feature consists of 4 components. Our model calculates the local blur feature based on image patches too, but we need only one scale and our local blur feature consists of 2 components. As a result, if the computational cost of each local blur feature component is consistent, the time cost of the model in literature [12] is at least 6 times as much as that of our proposed model. That is, the proposed method can realize simple and effective motion blurred region detection.

G. RESTORATION OF LOCAL MOTION BLURRED IMAGE

A local blur image is used to evaluate the effectiveness of the proposed blur region detection method in the application of local motion blur image restoration, which is shown as figure 16. Figure 16(a) is the local motion blurred image; figure 16(b) and (c) are the clear and blur areas obtained by our proposed algorithm; figure 16(d) is the original image marked with a blue rectangle on a small clear region and a red rectangle on a small blur region; figure 16(e) is the restoration result by the algorithm proposed by Xu and Jia [22]; figure 16(f) is the restoration result obtained by blur region restoration based on our proposed method; figure 16(g) $\sim$ (i) are the enlarged regions corresponding to figure 16(d) $\sim$ (f). As can be seen from figure 16, compared with Xu's method, the blur regions restored by our proposed method are clearer, and the restored clear regions have no obvious ringing effect. The main reason is that for the local motion blurred image of a single moving target, the motion situation of the foreground and background in the image is inconsistent. If this kind of image is directly processed by the consistency restoration algorithm as reference [22], serious visual artifacts will be generated in the clear area of the image. Therefore, the blur images are divided into blur region and clear region according to our proposed algorithm, and then the consistent deblurring algorithm [23] is adopted to restore the blur region. The final restoration image can be obtained by mosaicking the restored blur region with the clear region.

That is, the proposed algorithm can be effectively applied to local motion blur image restoration.

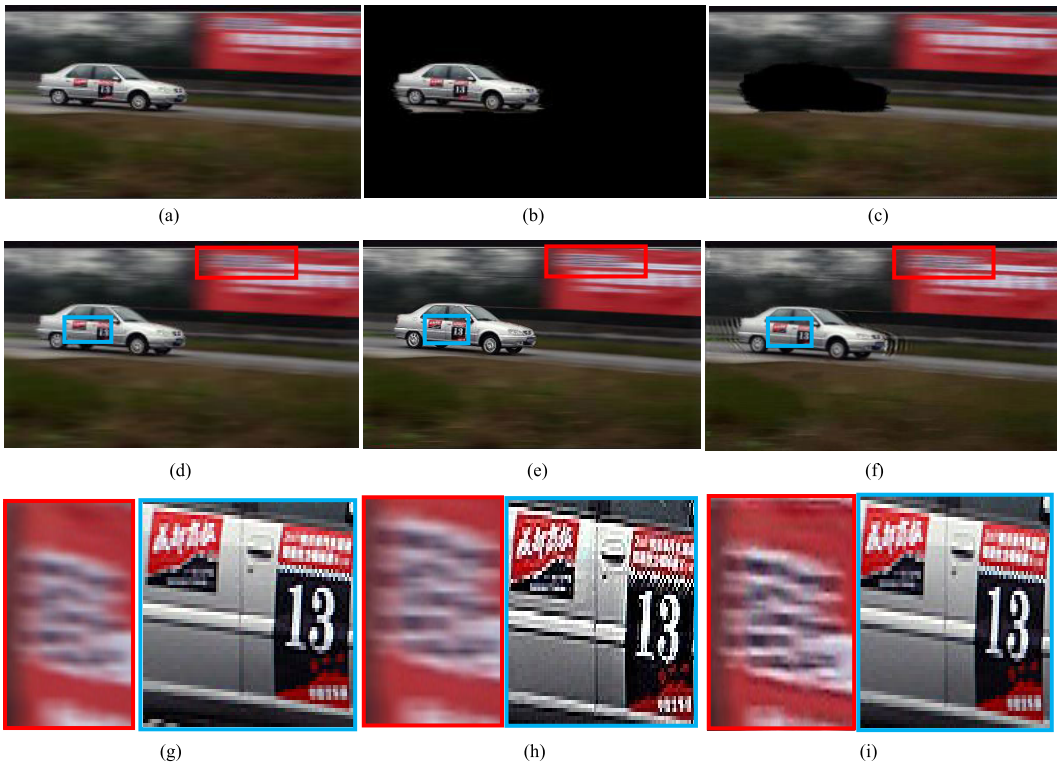

FIGURE 16. Local motion blurred image restoration. (a) Input local blurred image; (b) Clear region determined by our proposed method; (c) Blur region determined by our proposed method; (d) Marked input image; (e) Restoration result of Xu's method [22]; (f) Restoration result by our proposed method; (g) Enlarged regions corresponding to (d); (h) Enlarged regions corresponding to (e); (i) Enlarged regions corresponding to (f); (g) local magnification of the Input image; (h) Local magnification of Xu's restoration result; (i) Local magnification of our restoration result.

V. CONCLUSION

To deal with the serious visual artifacts caused by the consistent restoration algorithm on local motion blurred images, a blur region detection algorithm based on a new blur discriminant criteria and automatic KNN matting is proposed. The algorithm consists of coarse blur detection and blur region refinement. The main contributions of the proposed method include two aspects. On one hand, a blur discriminant criteria involving blur characteristics in frequency domain and spatial domain is designed to realize coarse localization of blur regions. The two kinds of blur features are relatively simple and have strong blur detection ability. Meanwhile, the proposed blur extraction criteria does not require multi-scale blur feature extraction and the computational complexity is low. On the other hand, an automatic KNN matting algorithm is proposed and used on the coarse blur region detection results to achieve blur areas refinement. This process avoids manual calibration process in the original KNN matting, and achieves the automatic detection and refinement of local motion blurred regions. Experimental results show that the proposed method is effective for local motion blurred image detection.

However, due to the direct mosaic of the clear region and the restored blur region, the inserted result still has some ringing effect on the boundary of the clear and blur region. In our subsequent work, we will focus on the smoothing effect on the boundary of the two regions.

ACKNOWLEDGMENT

The authors would like to thank anonymous reviewers for their valuable comments.

REFERENCES

[1] B. Ma, L. Huang, J. Shen, L. Shao, M.-H. Yang, and F. Porikli, "Visual tracking under motion blur," *IEEE Trans. Image Process.*, vol. 25, no. 12, pp. 5867–5876, Dec. 2016.

[2] T. Jha, "Velocity detection from a motion blur image using radon transformation," *Proc. TUJ*, vol. 32, no. 2, pp. 243–248, Dec. 2018.

[3] J. A. Cortés-Osorio, J. B. Gómez-Mendoza, and J. C. Riaño-Rojas, "Velocity estimation from a single linear motion blurred image using discrete cosine transform," *IEEE Trans. Instrum. Meas.*, vol. 68, no. 10, pp. 4038–4050, Oct. 2019.

[4] X. Qi, C.-G. Li, G. Zhao, X. Hong, and M. Pietikäinen, "Dynamic texture and scene classification by transferring deep image features," *Neurocomputing*, vol. 171, pp. 1230–1241, Jan. 2016.

[5] S. Li, B. Seybold, A. Vorobyov, X. Lei, and C.-C. J. Kuo, "Unsupervised video object segmentation with motion-based bilateral networks," in *Proc. Eur. Conf. Comput. Vis. (ECCV)*, Sep. 2018, pp. 207–223.

[6] P. Bideau and E. Learned-Miller, "It's moving! A probabilistic model for causal motion segmentation in moving camera videos," in *Proc. Eur. Conf. Comput. Vis. (ECCV)*, 2016, pp. 433–449.

[7] S. A. Golestaneh and L. J. Karam, "Spatially-varying blur detection based on multiscale fused and sorted transform coefficients of gradient magnitudes," in *Proc. IEEE Conf. Comput. Vis. Pattern Recogn. (CVPR)*, Jul. 2017, pp. 5800–5809.

[8] X. Wang, X. Liang, J. Zheng, and H. Zhou, "Fast detection and segmentation of partial image blur based on discrete Walsh-Hadamard transform," *Signal Process., Image Commun.*, vol. 70, pp. 47–56, Feb. 2019.

[9] C. Tang, J. Wu, Y. Hou, P. Wang, and W. Li, "A spectral and spatial approach of coarse-to-fine blurred image region detection," *IEEE Signal Process. Lett.*, vol. 23, no. 11, pp. 1652–1656, Nov. 2016.

[10] B. Su, S. Lu, and C. L. Tan, "Blurred image region detection and classification," in *Proc. 19th ACM Int. Conf. Multimedia*, Scottsdale, AZ, USA, 2011, pp. 1397–1400.
[11] R. Liu, Z. Li, and J. Jia, "Image partial blur detection and classification," in *Proc. IEEE Conf. Comput. Vis. Pattern Recogt. (CVPR)*, Anchorage, AK, USA, Jun. 2008, pp. 954–961.
[12] J. Shi, L. Xu, and J. Jia, "Discriminative blur detection features," in *Proc. IEEE Conf. Comput. Vis. Pattern Recogn. (CVPR)*, Columbus, OH, USA, Jun. 2014, pp. 2965–2972.
[13] K. Bahrami, A. C. Kot, and J. Fan, "A novel approach for partial blur detection and segmentation," in *Proc. IEEE Int. Conf. Multimedia Expo (ICME)*, San Jose, CA, USA, Jul. 2013, pp. 1–6.
[14] T.-L. Wang, K.-Y. Lee, and Y.-C. F. Wang, "Partial image blur detection and segmentation from a single snapshot," in *Proc. IEEE Int. Conf. Acoust. Speech Signal Process. ICASSP*, Mar. 2017, pp. 1907–1911.
[15] S. Dai and Y. Wu, "Removing partial blur in a single image," in *Proc. IEEE Conf. Comput. Vis. Pattern Recogn. (CVPR)*, Jun. 2009, pp. 2544–2551.
[16] R. Kohler, M. Hirsch, B. Schölkopf, and S. Harmel-ing, "Improving alpha matting and motion blurred foreground estimation," in *Proc. IEEE Int. Conf. Image Process. (ICIP)*, Sep. 2013, pp. 3446–3450.
[17] J. Zhao, H. Feng, Z. Xu, Q. Li, and X. Tao, "Automatic blur region segmentation approach using image matting," *Signal, Image Video Process.*, vol. 7, no. 6, pp. 1173–1181, 2013.
[18] Q. Chen, D. Li, and C. K. Tang, "KNN matting," *IEEE Trans. Pattern Anal. Mach. Intell.*, vol. 35, no. 9, pp. 2175–2188, Sep. 2013.
[19] R. C. Gonzalez and R. E. Woods, *Digital Image Processing*, 3rd ed. Upper Saddle River, NJ, USA: Prentice-Hall, 2008.
[20] T. Porter and T. Duff, "Compositing digital images," in *Proc. 11th Annu. Conf. Comput. Graph. Interact. Techn. (SIGGRAPH)*, New York, NY, USA, 1984, pp. 253–259.
[21] B. Amin, M. M. Riaz, and A. Ghafoor, "A hybrid defocused region segmentation approach using image matting," *Multidimensional Syst. Signal Process.*, Vol. 30, no. 2, pp. 561–569, Apr. 2019.
[22] L. Xu and J. Jia, "Two-phase kernel estimation for robust motion deblurring," in *Proc. Eur. Conf. Comput. Vis, (ECCV)*, 2010, pp. 157–170.
[23] J. Pan, D. Sun, H. Pfister, and M.-H. Yang, "Blind image deblurring using dark channel prior," in *Proc. IEEE Conf. Comput. Vis. Pattern Recognit. (CVPR)*, Jun. 2016, pp. 1628–1636.

MINGHUA ZHAO received the Ph.D. degree in computer science from Sichuan University, Chengdu, China, in 2006. After that, she joined the Xi'an University of Technology, Xi'an, China. She is currently a Professor with the School of Computer Science and Engineering, Xi'an University of Technology. Her research interests include computer graphics, human–computer interaction, image processing, pattern recognition, and computer vision.

DAN LI received the B.S. degree in software engineering from the Guangxi University of Science and Technology, Liuzhou, China, in 2017. She is currently pursuing the degree with the School of Computer Science and Engineering, Xi'an University of Technology, Xi'an, China. Her research interests include computer vision, image processing, and deep learning.

ZHENGHAO SHI received the Ph.D. degree in computer architecture from the Xi'an Institute of Micro-Electronics, Xi'an, China, in 2005. In 2000, he joined the Xi'an University of Technology, Xi'an. He is currently an Associate Professor with the School of Computer Science and Engineering, Xi'an University of Technology. His research interests include image processing, pattern recognition, and computer-aided diagnosis.

SHUANGLI DU received the Ph.D. degree in computer science from Sichuan University, in 2017. In 2014, she was a Visiting Student with the Agency for Science, Technology and Research (A∗STAR), Singapore. Her research interests include low-rank decomposition, computer vision, and pattern recognition.

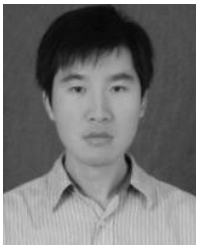

PENG LI received the M.S. degree in computer science and technology from Xidian University, China, in 2006. After that, he joined the Xi'an University of Technology, Xi'an, China. He is currently a Lecturer with the School of Computer Science and Engineering, Xi'an University of Technology. His research interests include computer architecture, image processing, and computer vision.

JING HU received the B.S. degree in software engineering from Nanchang University, Nanchang, China, in 2013, and the Ph.D. degree in communication and information systems from Xidian University, Xi'an, China, in 2018. She is currently a Teacher with the School of Computer Science and Technology, Xi'an University of Technology. Her research interests include image processing and deep learning.